

# Renormalisation Scale Dependencies in Dijet Production at HERA

T. Carli Max-Planck-Institut für Physik, München, Germany<sup>1</sup>

**Abstract:** Different choices of the renormalisation scale ( $\mu_{ren}$ ) can be used to describe hard scattering processes with two jets at large transverse momentum in deep-inelastic scattering at HERA by fixed order perturbative QCD calculations. For leading (LO) and next-to-leading order (NLO) calculations the simplest choices,  $Q^2$ , the virtuality of the incoming photon, and the mean squared transverse momenta of the two jets  $E_T^2$ , are studied in different kinematic regimes. It is found that only if both  $Q^2$  and  $E_T^2$  are large, the NLO calculation is stable with respect to numerical variations of  $\mu_{ren}$  while the LO calculation strongly depends on it. If only one of the two scales, either  $Q^2$  or  $E_T^2$ , is large, the NLO is more stable than the LO calculation, but exhibits nevertheless a strong residual scale dependence. When both scales are relatively small, large scale dependencies are found in both cases. Moreover, large differences between the LO and NLO calculation are found.

Generally, the use of  $E_T^2$  as renormalisation scale is favoured over  $Q^2$ , since scale dependencies are less pronounced and NLO corrections are smaller.

## 1 Introduction

HERA colliding 27.5 GeV positrons on 820 GeV proton offers an ideal testing ground for perturbative QCD (pQCD) in deep-inelastic scattering (DIS). The centre of mass energy of  $\sqrt{s} \approx 300$  GeV leads to a large phase space for hadron production and to the possibility to observe collimated sprays of hadrons - called jets - in the hadronic final state. They are the experimentally accessible signs of a hard scattering process and relate the fundamental objects of pQCD, the unobservable quarks and gluons, to the measurable hadronic final state.

At HERA, events with two jets in the central part of the detector can be produced in quark ( $q\gamma \rightarrow qg$ ) or gluon ( $g\gamma \rightarrow q\bar{q}$ ) initiated hard subprocesses (see Fig. 1). In fixed order pQCD the dijet cross section can be written as:

$$\frac{d^2\sigma_{dijet}}{dx dQ^2} \sim \sum_n \alpha_s^n(\mu_{ren}^2) \int_0^1 \frac{d\xi}{\xi} C_n(x/\xi, \mu_{ren}^2, \mu_{fac}^2, \dots) \cdot PDF(\xi, \mu_{fac}^2) \quad (1)$$

The variables  $x$  and  $Q^2$  are the usual variables to inclusively describe DIS (see Fig. 1 for definition). The (non-perturbative) universal parton density functions of the incoming proton  $PDF$  are evaluated at the factorisation scale  $\mu_{fac}^2$ . They further depend on  $\xi = x (1 + \hat{s}/Q^2)$ , where  $\sqrt{\hat{s}}$  is the invariant mass of the hard partonic system. The variable  $\xi$  can be interpreted as the fractional momentum of the parton initiating the hard subprocess with respect to the proton momentum. In leading order, where  $\hat{s}$  is the invariant mass of the dijet system,  $\xi$  can be directly measured once the dijet system is tagged. The coefficient functions  $C_n$  can be calculated in pQCD as power series expansions in the strong coupling constant  $\alpha_s(\mu_{ren}^2)$  probed at the squared renormalisation scale  $\mu_{ren}^2$ .

<sup>1</sup> Contribution to the Proceedings of the DESY Workshop 1998/99 on Monte Carlo Generators for HERA Physics.

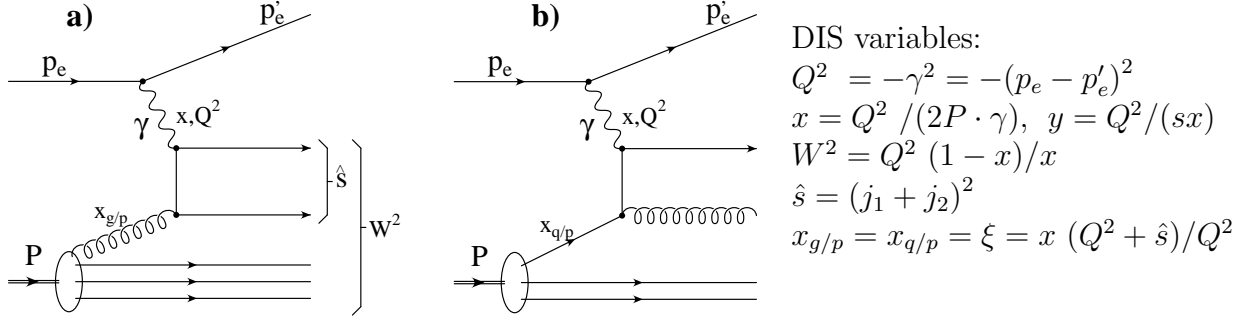


Figure 1: *Feynman diagrams for the production of dijet events to first order of  $\alpha_s$  in  $e^\pm p$  - collisions.  $\gamma$  ( $P$ ) denotes the four-momentum of the photon (proton).  $j_1$  and  $j_2$  are the four-momenta of the jets associated to the hard subprocess.*

The dijet cross section including higher order parton emissions are difficult to calculate using exact expressions for the coefficient functions. Since the phase space integrals cannot be solved analytically, numerical methods have to be applied. Several Monte Carlo integration programs are available to compute jet cross sections in next-to-leading order (NLO) of  $\alpha_s$  (MEPJET [1, 2], JETVIP [3], DISENT [4, 5] and DISASTER [6]). They have been carefully compared in this workshop [7]. They allow any jet definition scheme and arbitrary experimental cuts to be analysed. In this article all results are based on the DISENT program. NLO (LO) calculations are performed using the CTEQ4M (CTEQ4L) parton density functions [8]. The value of  $\alpha_s$  is taken from the parton density functions. In CTEQ4L  $\alpha_s(M_Z) = 0.131$  and in CTEQ4M  $\alpha_s(M_Z) = 0.116$  is used. The factorisation scale has been set to  $\mu_{fac}^2 = Q^2$ . The dependencies of the results presented here on the factorisation scales are small and can be neglected.

## 2 Choice of the Renormalisation Scale in DIS

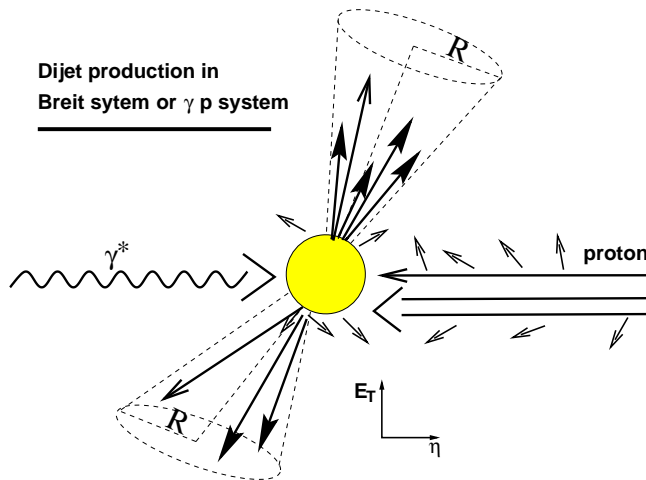


Figure 2: *Diagram for the production of dijet events in the Breit or hcms frame in DIS.*

process:  $Q^2$ , the virtuality of the incoming photon, as used in the QCD analysis of the inclusive

<sup>2</sup>e.g. the hadronic centre of mass (hcms) frame defined by  $\vec{\gamma} + \vec{P} = 0$  or the Breit frame defined by  $\vec{\gamma} + 2x \vec{P} = 0$ . In the laboratory frame and in the Breit frame the proton moves towards the  $+z$  direction.

DIS cross section, or the mean squared transverse momenta of the two jets  $E_T^2$  as used in hadron-hadron collisions. In this article the behaviour of the dijet cross section in different kinematic regimes for both  $Q^2$  and  $E_T^2$  as nominal renormalisation scales is investigated.

To decide whether a physical process is probed at its natural scale and whether the pQCD prediction can be expected to be stable, the following criteria could give some guidance. The NLO corrections, i.e. the ratio of the NLO to the LO cross section, the so-called K-factor, should not be too large, since in this case it is conceivable that corrections of the next-to-next-to-leading order can be large. The residual scale dependence, i.e. the variation of the cross section when changing the nominal squared renormalisation scale ( $\mu_{nom}^2$ ) by about an order of magnitude using a scale factor  $1/4 \leq \xi_{ren} \leq 4$ , should be small ( $\mu_{ren}^2 = \xi_{ren} \cdot \mu_{nom}^2$ ). Moreover, the NLO calculation should depend less on variations of  $\xi_{ren}$ .

### 3 Dijet Rates and Cut Scenario

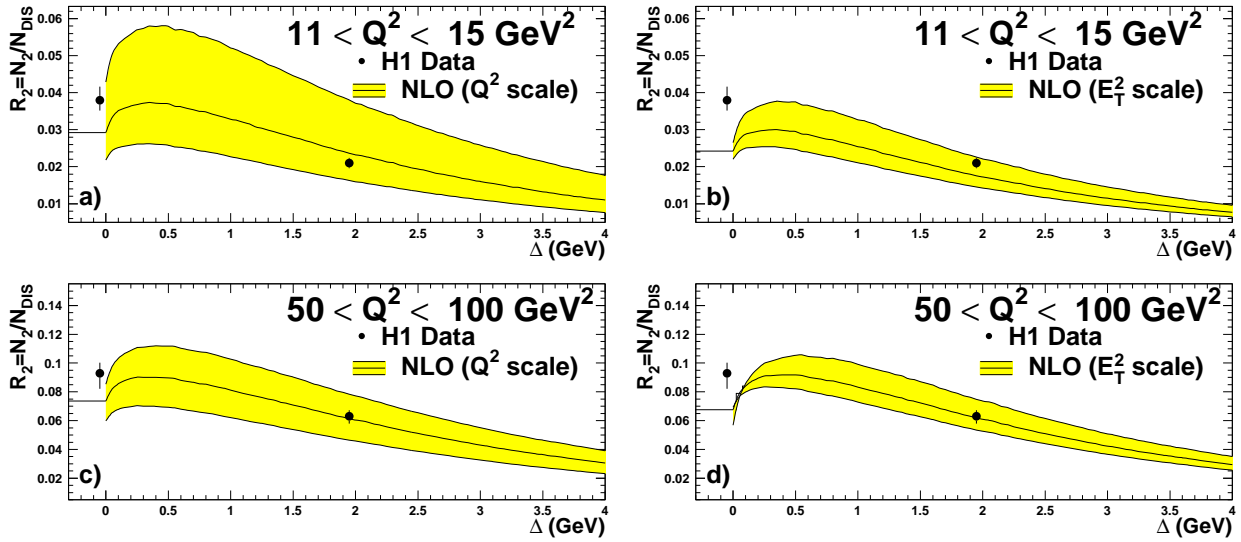


Figure 3: Dijet rate  $R_2 = N_2/N_{DIS}$  as a function of the threshold difference  $\Delta$  of the first and second jet. Jets are defined by the cone algorithm ( $R_{cone} = 1$ ) in the hadronic centre of mass system with  $E_{T2} \geq 5$  GeV and  $E_{T1} \geq 5 + \Delta$  GeV. Shown are H1 data (points) for  $11 \leq Q^2 \leq 15$  GeV<sup>2</sup> (a,b) and  $50 \leq Q^2 \leq 100$  GeV<sup>2</sup> (c,d) together with a NLO QCD calculation (line) with  $Q^2$  (a,c) and the mean  $E_T^2$  (b,d) as renormalisation scale  $\mu_{nom}^2$ . The shaded band indicates the variation of the NLO prediction for  $4 \cdot \mu_{nom}^2$  and  $1/4 \cdot \mu_{nom}^2$ .

Before studying the scale dependencies of the dijet cross section, it is first indispensable to find a cut scenario where pQCD can describe the data. For dijet production in DIS this has been a problem at HERA. For a long time agreement with NLO calculations could only be achieved in very restricted phase space regions (see e.g. [9]). Especially in the region of low  $Q^2 \lesssim 50$  GeV<sup>2</sup>, NLO calculations failed to describe the data. Meanwhile, it has been understood that this discrepancy occurs when both jets are required to be above the same  $E_T$  threshold. As  $\Delta$  defined as the required  $E_T$  difference of the threshold of the two leading jets, approaches 0, a fixed order calculation gets infra-red sensitive [10, 11, 12]. In this region a reliable prediction of the jet cross section is not possible with a fixed order calculation.

This has been demonstrated in an analysis by the H1 collaboration [13], where  $R_2 = N_2/N_{DIS}$ , the ratio of the two jet cross section to the inclusive DIS cross section, has been

measured in the region<sup>3</sup>  $5 \leq Q^2 \leq 100 \text{ GeV}^2$ ,  $156^\circ \leq \theta_{el} \leq 173^\circ$ ,  $E_{el} \geq 11 \text{ GeV}$  and  $y \geq 0.05$ . Jets are defined in the hadronic centre of mass system by the cone algorithm [14] with a radius  $R_{cone} = 1$ . The  $E_T$  of the second jet is required to be  $E_{T2} \geq 5 \text{ GeV}$  and the  $E_T$  of the first jet  $E_{T1} \geq 5 + \Delta \text{ GeV}$ , where  $\Delta$  is set to 0 or 2 GeV. The difference of their pseudo-rapidities<sup>4</sup> should be  $|\eta^*| < 2$ .

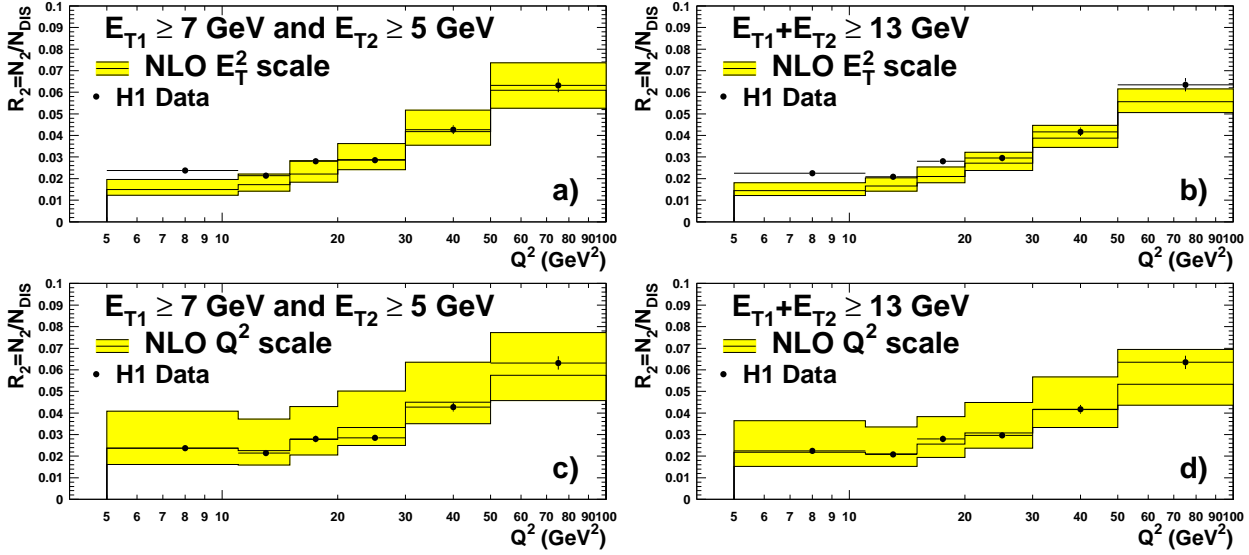


Figure 4: Dijet rate  $R_2 = N_2/N_{DIS}$  as a function of  $Q^2$ . Jets are defined by the cone algorithm ( $R_{cone} = 1$ ) in the hadronic centre of mass system with  $E_{T2} \geq 5 \text{ GeV}$  and  $E_{T1} \geq 7 \text{ GeV}$  (a,c) or  $E_{T2} + E_{T1} \geq 13 \text{ GeV}$  (b,d). Shown are H1 data (points) together with a NLO QCD calculation (line) with  $Q^2$  (c,d) and the mean  $E_T^2$  (a,b) as renormalisation scale  $\mu_{nom}^2$ . The shaded band indicates the variation of the NLO prediction for  $4 \cdot \mu_{nom}^2$  and  $1/4 \cdot \mu_{nom}^2$ .

The data points for  $11 \leq Q^2 \leq 15 \text{ GeV}^2$  (a,b) and  $50 \leq Q^2 \leq 100 \text{ GeV}^2$  (c,d) are shown in Fig. 3. As expected, in the data the dijet rate is higher at  $\Delta = 0 \text{ GeV}$  than it is at  $\Delta = 2 \text{ GeV}$ . In the NLO calculation the expected rise of the dijet rate towards decreasing  $\Delta$  is also visible. However, around  $\Delta \approx 0.5 \text{ GeV}$  the calculated dijet rate turns around and falls down until  $\Delta \approx 0 \text{ GeV}$  is reached. Around this point the NLO cross section falls with an infinite slope [10], but remains finite. In this region the  $E_T$  of the jets are approximately equal and no phase space is available to emit a third real parton. This leads to an incomplete cancellation between real and virtual corrections at the threshold and makes a fixed order calculation unpredictable. A resummation of higher orders is necessary at this phase space point. Since the virtual corrections give a negative contribution, the dijet rate artificially drops down in the NLO calculation. The problem only occurs for events containing two jets with balanced momenta. In such a configuration the emission of a real third parton would lead to a configuration where one parton is above the  $E_T$  threshold and the other below. If the thresholds of the two jets are different, the event has either balanced jet momenta or has jets with one above and the other below the thresholds. Since these conditions are never fulfilled at the same time, no problem occurs.

In Fig. 3 one can see that the point  $\Delta = 2 \text{ GeV}$  is well described by the calculation while

<sup>3</sup>  $\theta_{el}$  ( $E_{el}$ ) is the polar angle (energy) of the scattered electron.

<sup>4</sup> The pseudo-rapidity is defined as  $\eta = -\ln \tan \theta/2$ . In the laboratory and in the Breit frame the proton moves into the  $+z$  direction.

for  $\Delta = 0$  GeV the calculation is below the data. This behaviour is independent of the used renormalisation scale. However, when  $Q^2$  is used a renormalisation scale a much larger scale dependence is found. In Fig. 4a and 4c it is demonstrated that the NLO calculation agrees well with the data for  $5 \leq Q^2 \leq 100$  GeV<sup>2</sup>, if  $\Delta = 0$  GeV is avoided. Hadronisation corrections would lower the NLO prediction by about 10 – 20%. Only in the case of the lowest  $Q^2$  bin the NLO calculation falls below the data. The difficult phase space region can not only be avoided by a cut on  $\Delta$ , but also by a cut on the sum of the two jets, e.g.  $E_{T1} + E_{T2} \geq 13$  GeV (see Fig. 4b and 4d). For both cut scenarios the  $Q^2$  scale exhibits a much larger scale dependence than the  $E_T^2$  scale (where  $E_T = (E_{T1} + E_{T2})/2$ ). The variation of the NLO calculation when changing the renormalisation scale by a factor of 4 up and down is illustrated as grey band. The central value for a scale factor of  $\xi_{ren} = 1$  is given as solid line. For both choices of scales,  $Q^2$  and  $E_T^2$ , the cut on the sum of the two jets leads to a slightly smaller scale dependence than the  $\Delta = 2$  GeV cut.

## 4 Dijet Cross Sections and their NLO Behaviour

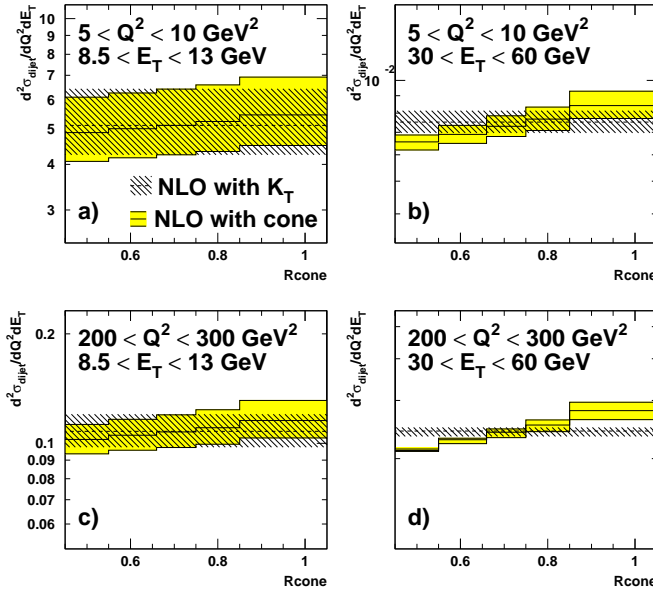


Figure 5: Dependence of the double differential dijet cross section  $d^2\sigma_{dijet}/dQ^2dE_T$  defined by the cone algorithm with a cone size of  $R_{cone}$  as calculated by NLO QCD ( $E_T^2$  scale) in different bins of  $Q^2$  and of the mean  $E_T$  in the Breit frame. The shaded band indicates the variation of the NLO prediction for  $4 \cdot \mu_{nom}^2$  and  $1/4 \cdot \mu_{nom}^2$ . Overlaid as hatched band is the cross section defined by the inclusive  $K_T$  algorithm always for  $R = 1$ . Jets are defined in the Breit frame with  $E_{T1} \geq E_{T2} \geq 5$  GeV,  $E_{T1} + E_{T2} \geq 17$  GeV and  $-1 \leq \eta_{lab} \leq 2.5$ .

Only at large  $E_T$  small cone sizes lead to improved scale dependencies. For

To investigate the interplay between the  $Q^2$  and the  $E_T^2$  scales in more detail, the following cut scenario is adopted. All jets lying well within the detector acceptance  $-1.5 \leq \eta_{lab} \leq 2.5$  are ordered in energy. Then the two highest  $E_T$  jets are required to fulfil:  $E_{T1} \geq E_{T2} \geq 5$  GeV and  $E_{T1} + E_{T2} \geq 17$  GeV. Jets are defined by the inclusive  $K_T$  algorithm [15, 16] in the Breit system. The kinematic phase space is defined by  $0.2 \leq y \leq 0.6$  and  $5 \leq Q^2 \leq 600$  GeV<sup>2</sup>. These cuts are very close to the ones used by the H1 collaboration in a recent extraction of the gluon density [17].

In a NLO calculation similar results are obtained with the inclusive  $K_T$  algorithm and with the cone algorithm with a cone size  $R_{cone} = 0.7$ . This is illustrated in Fig. 5 where the total dijet cross section  $d^2\sigma_{dijet}/dQ^2dE_T$  in two  $Q^2$  and mean  $E_T = (E_{T1} + E_{T2})/2$  bins<sup>5</sup> is shown as a function of the cone size  $R_{cone}$  used in the cone algorithm<sup>6</sup>. In case of the cone algorithm the scale dependence is only slightly influenced by

<sup>5</sup>Here and in the following figures,  $d^2\sigma_{dijet}/(dQ^2dE_T)$  is the total dijet cross section integrated over a  $Q^2$  and  $E_T$  bin and divided by the bin width.

<sup>6</sup>For the  $K_T$  algorithm the distance parameter  $R$  is always set to 1. For an exact definition see ref. [18].

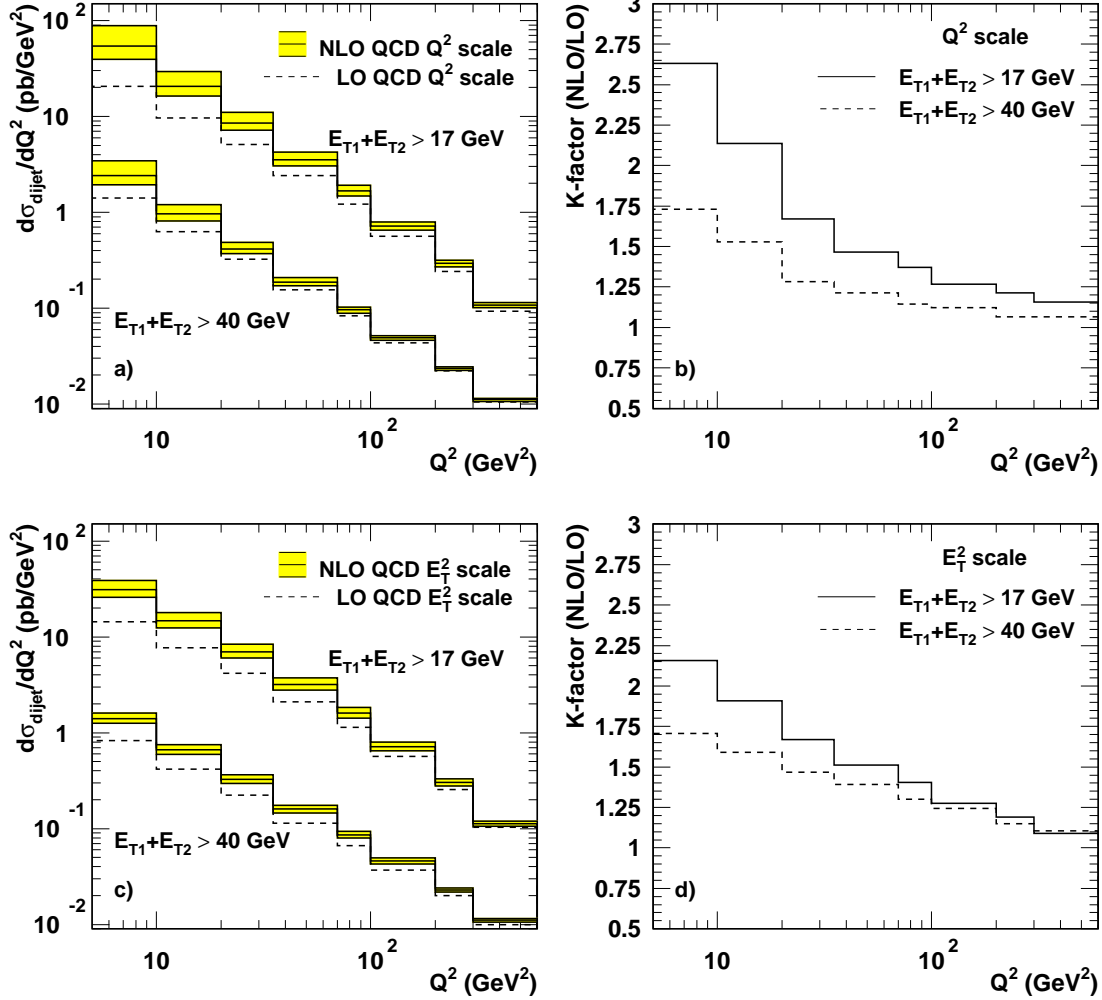


Figure 6: *Dijet cross section as a function of  $Q^2$  as calculated by NLO (line) and LO (dashed line) QCD using  $Q^2$  (a) or the mean  $E_T^2$  (c) as renormalisation scale  $\mu_{\text{ren}}^2$ . The shaded band indicates the variation of the NLO prediction for  $4 \cdot \mu_{\text{nom}}^2$  and  $1/4 \cdot \mu_{\text{nom}}^2$ . The ratio of the NLO to the LO calculation is shown in (b) and (d). Jets are defined by the inclusive  $K_T$  algorithm in the Breit frame with  $E_{T1} \geq E_{T2} \geq 5$  GeV and  $-1 \leq \eta_{\text{lab}} \leq 2.5$ . Shown are cross sections for  $E_{T1} + E_{T2} \geq 17$  GeV and  $E_{T1} + E_{T2} \geq 40$  GeV.*

$R_{\text{cone}} = 0.7$  both jet algorithms exhibit the same scale dependence. However, the inclusive  $K_T$  algorithm is defined in a less ambiguous way and is better suited for NLO comparisons with data [19, 20, 21]. Therefore the inclusive  $K_T$  jet algorithm is the preferred choice and is used in the following.

In Fig. 6a ( $Q^2$  scale) and 6c ( $E_T^2$  scale) the inclusive dijet cross section is shown as a function of  $Q^2$  for  $E_{T1} + E_{T2} \geq 17$  GeV and  $E_{T1} + E_{T2} \geq 40$  GeV. At low  $Q^2$  where  $E_T^2$  is higher than  $Q^2$  the corresponding cross section calculated with  $E_T^2$  as scale is lower, since  $\alpha_s$  is probed at a higher scale. Starting at  $Q^2 \gtrsim 40$  GeV<sup>2</sup> the dijet cross section is of comparable size for both scales. For both  $E_T$  cuts, the scale dependence is largest at lowest  $Q^2$ . The K-factor shows a similar behaviour (see Fig. 6b and Fig. 6d). When using  $Q^2$  as scale, at  $Q^2 \approx 10$  GeV<sup>2</sup> for  $E_{T1} + E_{T2} \geq 17$  GeV ( $E_{T1} + E_{T2} \geq 40$  GeV) the LO cross section is about a factor of 2 (1.75)

below the NLO cross section. Only at the largest  $Q^2$  of 600  $\text{GeV}^2$  the NLO correction is small, i.e. about 15% (5%). When using  $E_T^2$  as scale (see Fig. 6c and Fig. 6d), the scale dependence is generally reduced and the K-factor is smaller.

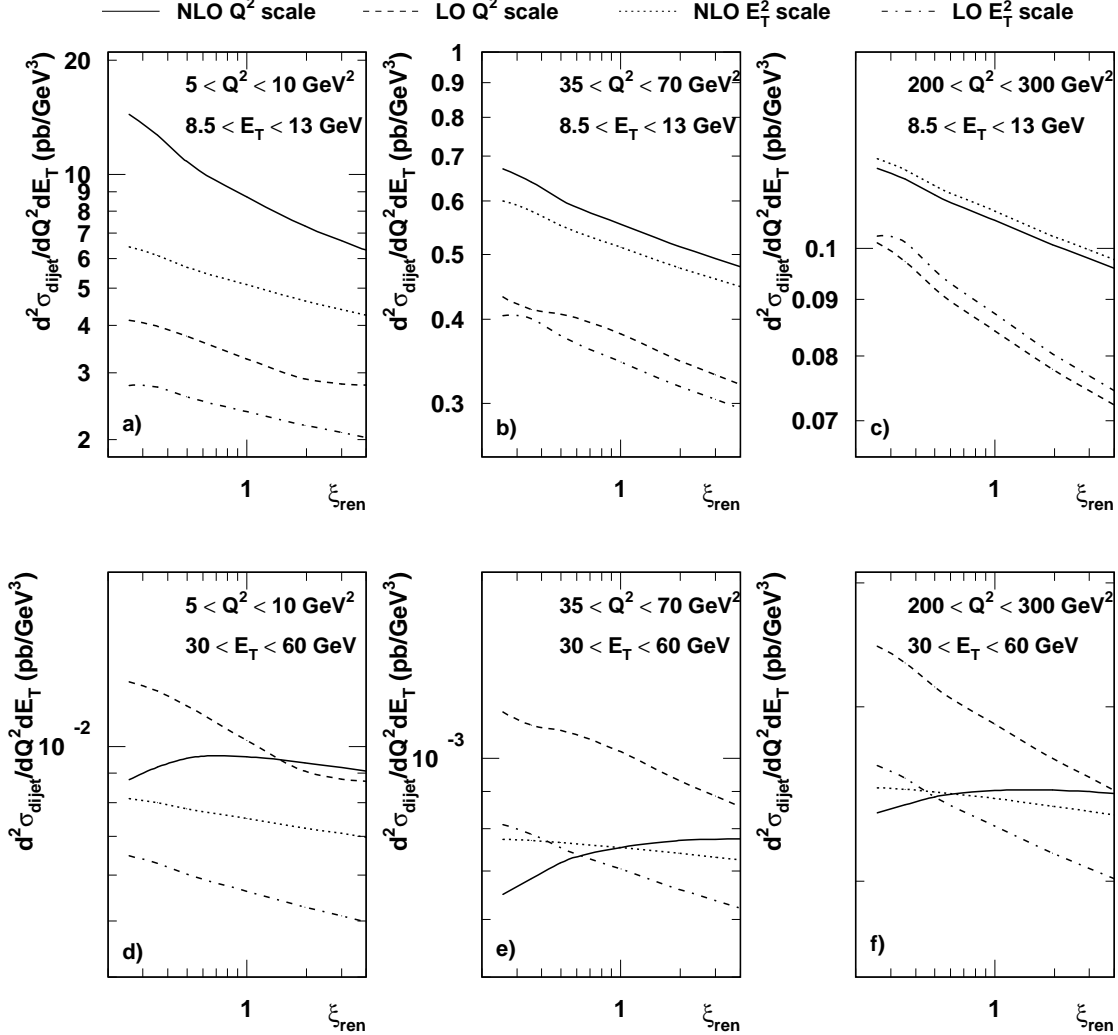


Figure 7: Double differential dijet cross section  $d^2\sigma_{\text{dijet}}/(dQ^2 dE_T)$  as a function of  $\xi_{\text{ren}}$  for different bins of  $Q^2$  and the mean  $E_T^2$ . Shown are NLO and LO QCD predictions for  $Q^2$  and the mean  $E_T^2$  as renormalisation scale  $\mu_{\text{ren}}^2 = \xi_{\text{ren}} \cdot \mu_{\text{nom}}^2$ . Jets are defined by the inclusive  $K_T$  algorithm in the Breit frame with  $E_{T1} \geq E_{T2} \geq 5 \text{ GeV}$ ,  $E_{T1} + E_{T2} \geq 17 \text{ GeV}$  and  $-1 \leq \eta_{\text{lab}} \leq 2.5$ .

The explicit dependence of the double differential dijet cross section on the scale factor  $\xi_{\text{ren}}$  is illustrated in Fig. 7 for three different bins in  $Q^2$  and mean  $E_T$ . Shown are the NLO and LO cross sections for  $Q^2$  and  $E_T^2$  as renormalisation scale.

For low  $Q^2$  ( $5 \leq Q^2 \leq 10 \text{ GeV}^2$ ) and low  $E_T$  ( $8.5 \leq E_T \leq 13 \text{ GeV}$ ) the NLO cross section exhibits a strong dependence on  $\xi_{\text{ren}}$  as is shown in Fig. 7a. It varies by a factor 2.5 for  $1/4 \leq \xi_{\text{ren}} \leq 4$  when  $Q^2$  is used as renormalisation scale. For the  $E_T$  scale this dependence is weaker (factor 1.6 for  $1/4 \leq \xi_{\text{ren}} \leq 4$ ), but still large. It is interesting that the LO cross section is more stable. It falls only by a factor of 1.5 for both the  $Q^2$  and the  $E_T^2$  scale. When the  $Q^2$  scale is replaced by the  $E_T^2$  scale, the cross section diminishes by a factor of 1.6 (1.2) in case



of NLO (LO). The K-factors are large, i.e. about a factor of 2 – 2.5, for both scales. The  $E_T^2$  scale leads to a slightly smaller K-factor.

Keeping  $E_T$  fixed at  $8.5 \leq E_T \leq 13$  GeV and increasing  $Q^2$  to  $200 \leq Q^2 \leq 300$  GeV<sup>2</sup>, gives the configuration displayed in Fig. 7c. Both choices of the renormalisation scale result in similar NLO and LO cross sections. The cross section is now slightly bigger in case of the  $E_T^2$  scale. The NLO cross section still reveals a distinct dependence on  $\xi_{ren}$ , but this dependence is now weaker than in the case of the LO cross section. The K-factors are reduced compared to the low  $Q^2$  result, but are still large (factor 1.5). At no value of  $\xi_{ren}$  the NLO and the LO cross section are similar.

Fig. 7d presents the results for  $5 \leq Q^2 \leq 10$  GeV<sup>2</sup> and  $30 \leq E_T \leq 60$  GeV. The dependence of the NLO cross section on  $\xi_{ren}$  is much reduced for both choices of scales. The LO cross section exhibits a much stronger dependence. For large  $E_T$  and  $5 \leq Q^2 \leq 300$  GeV<sup>2</sup> the LO cross section is higher than the NLO cross section when  $Q^2$  is used as scale. In case of the  $Q^2$  scale around  $\xi_{ren} \approx 2$  the K-factor is 1. This point moves to higher  $\xi_{ren}$  values as  $Q^2$  increases. In case of the  $E_T^2$  scale such a point is at very low  $\xi_{ren}$  values at low  $Q^2$  and is around  $\xi_{ren} = 1/2$  for  $35 \leq Q^2 \leq 300$  GeV<sup>2</sup>.

If both  $Q^2$  and  $E_T$  are large, the NLO cross sections are stable for both scale choices (see Fig. 7f). Moreover, the magnitude of the cross section is very similar for both scales. The LO cross section is steeply falling as  $\xi_{ren}$  increases. The K-factor is 1 for  $\xi_{ren} = 1/2$  ( $\xi_{ren} = 4$ ) in case of the  $E_T^2$  ( $Q^2$ ) scale.

It is interesting to note that the variation of the NLO cross section with the scale factor  $\xi_{ren}$  as well as the K-factor strongly depend on the position of the jets with respect to the proton. This is illustrated in Fig. 8 where the dijet cross section as a function of pseudo-rapidity of the forward jet in the laboratory frame  $\eta_{fwd,lab}$  is shown for three  $Q^2$  bins. Here  $E_T^2$  is used as renormalisation scale. In configurations where both jets are backward, i.e. small values of  $\eta_{fwd,lab}$ , small scale dependencies and K-factors around unity are found. However, as the forward jet moves towards the proton direction increasingly large scale factors are found. For  $5 \leq Q^2 \leq 10$  GeV<sup>2</sup> the NLO correction is 600% and even for  $200 \leq Q^2 \leq 300$  GeV<sup>2</sup> the NLO correction is still 300% ! Also the scale dependence of the NLO cross section gradually increases from about 30% for small  $\eta_{fwd,lab}$  to about 70% for large  $\eta_{fwd,lab}$  at low  $Q^2$ . Although somewhat smaller, the same effect is visible at large  $Q^2$ . These large K-factors suggest that NNLO corrections will be important. In the specific context of forward jet production studied in a more restricted phase space, this has already been demonstrated [22].

## 5 Conclusions

The behaviour of fixed order calculations in dijet production at HERA has been investigated. A cut scenario where the transverse energy of both jets are required to be above the same threshold has to be avoided to get agreement of the NLO calculation with the data. Dijet rates for  $5 \leq Q^2 \leq 100$  GeV<sup>2</sup> can be described by a NLO calculation when using the  $E_T^2$  or the  $Q^2$  scale. The  $E_T^2$  scale leads to smaller scale dependencies.

The interplay between the virtuality of the photon  $Q^2$  and the mean transverse energy of the dijet system in the Breit frame  $E_T^2$  has been studied in detail using dijet cross sections for  $5 \leq Q^2 \leq 600$  GeV<sup>2</sup> and  $8.5 \leq E_T \leq 60$  GeV as observable.



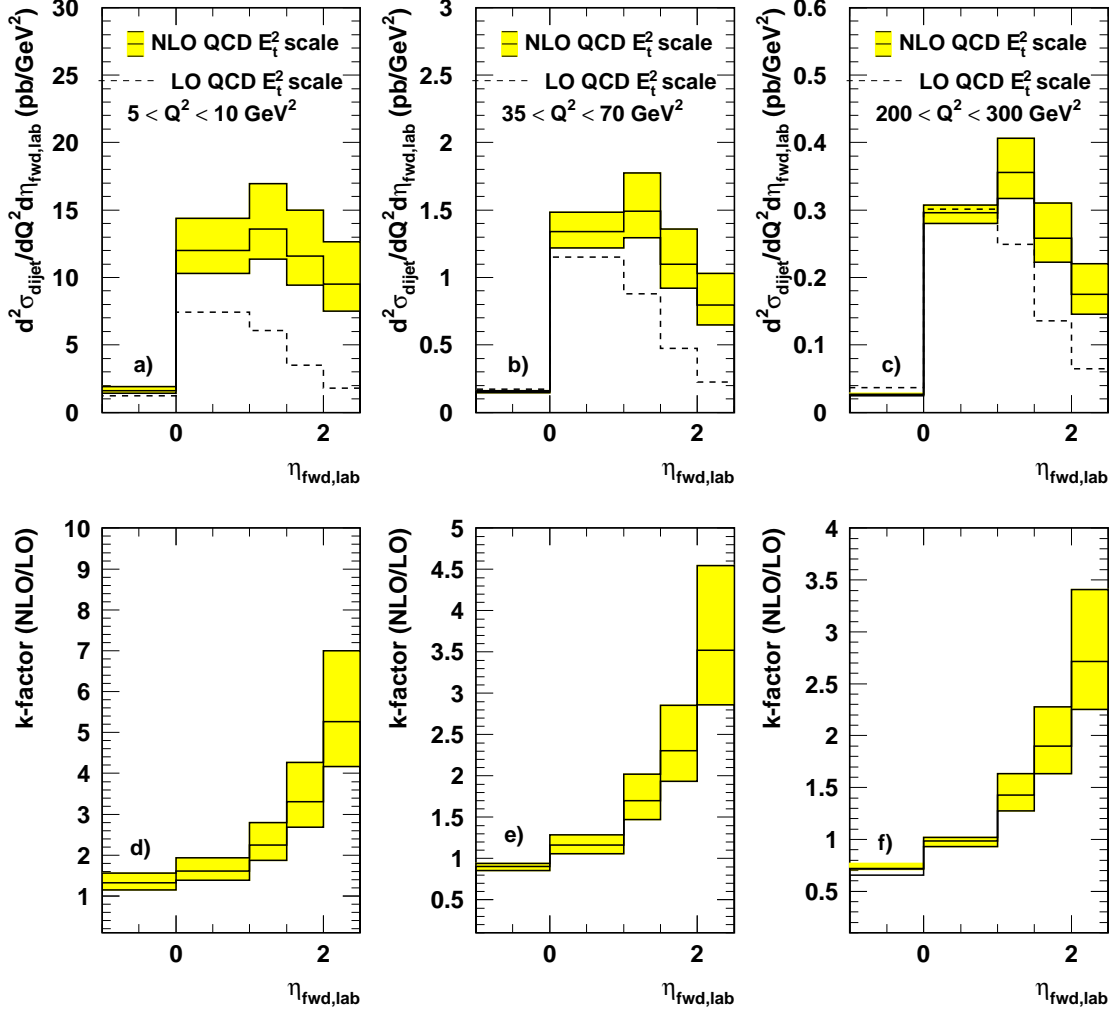


Figure 8: *Dijet cross section as a function of the pseudo-rapidity of the forward jet  $\eta_{fwd,lab}$  for different  $Q^2$  bins. Shown are NLO and LO QCD predictions for the mean  $E_T^2$  as renormalisation scale  $\mu_{nom}^2$ . The shaded band indicates the variation of the NLO prediction for  $4 \cdot \mu_{nom}^2$  and  $1/4 \cdot \mu_{nom}^2$ . Jets are defined by the inclusive  $K_T$  algorithm in the Breit frame with  $E_{T1} \geq E_{T2} \geq 5$  GeV,  $E_{T1} + E_{T2} \geq 17$  GeV and  $-1 \leq \eta_{lab} \leq 2.5$ .*

Only if both  $Q^2$  and  $E_T^2$  are large, the pQCD seems to make reliable predictions. The NLO calculation is independent of the renormalisation factor  $\xi_{ren}$  while the LO calculation strongly depends on it. Moreover, a point can be found where the NLO and the LO cross section have approximately the same size. If either  $Q^2$  or  $E_T^2$  is large and the other scale small, the NLO is more stable than the LO calculation, but exhibits nevertheless a dependence on  $\xi_{ren}$ . This is more pronounced, if  $Q^2$  is large and  $E_T^2$  small than in the opposite case where  $E_T^2$  is large and  $Q^2$  small. When both scales are relatively small, large scale dependencies are found. In this case a LO calculation seems to be more stable than the NLO calculation. Moreover, large NLO corrections are found.

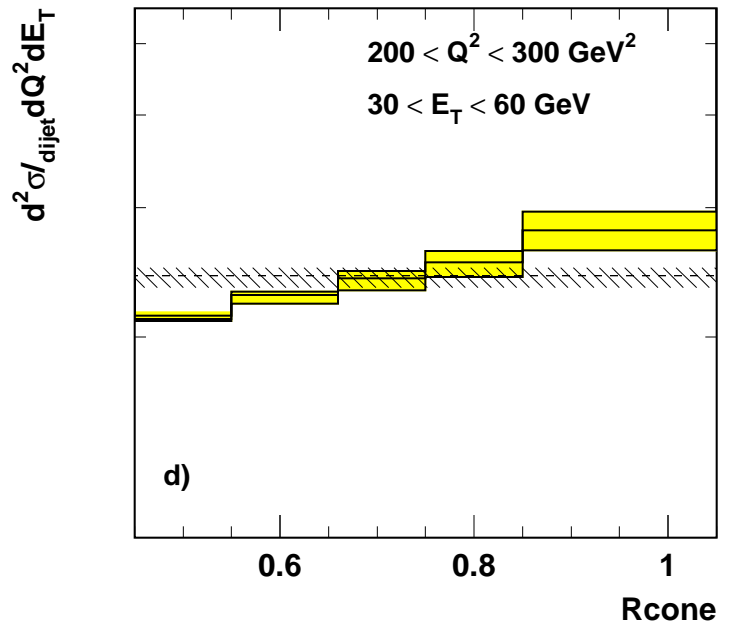
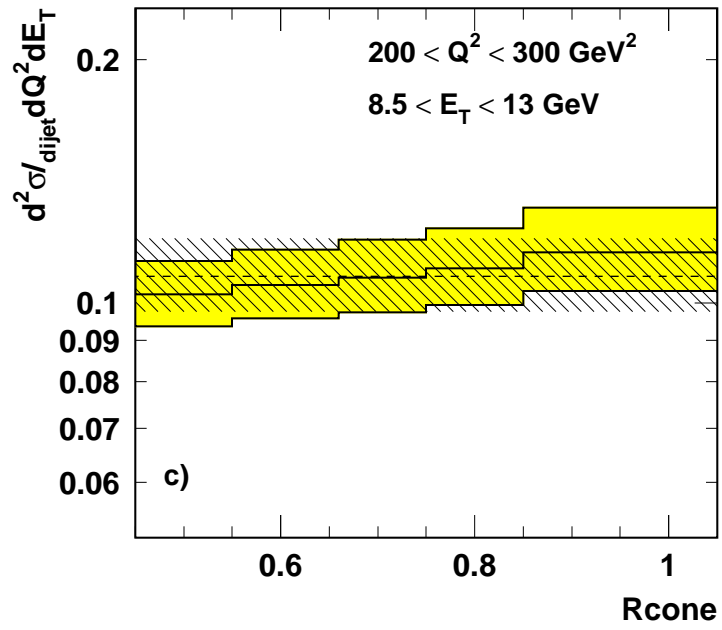
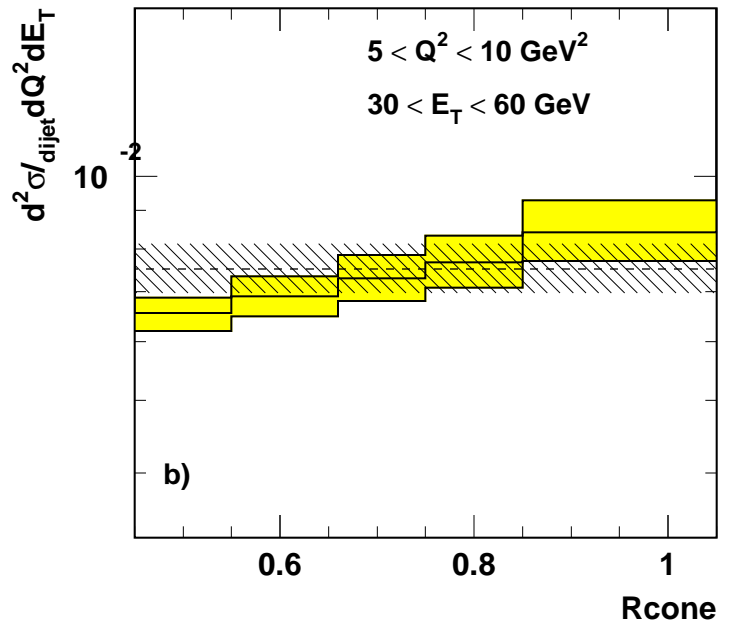
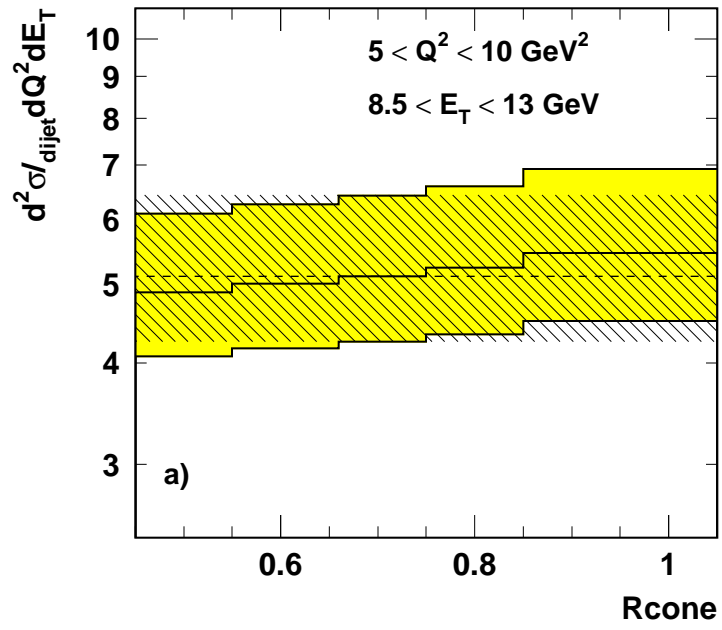
Generally, the use of  $E_T^2$  as renormalisation scale is favoured over  $Q^2$ , since scale dependencies are less pronounced and NLO corrections are smaller.

# Acknowledgments

I would like to thank my colleagues P. Pötter, T. Schörner, M.H. Seymour and D. Soper for the critical reading of the manuscript.

# References

- [1] E. MIRKES AND D. ZEPPENFELD, *Phys. Lett. B* 380 (1996) 105.
- [2] E. MIRKES AND D. ZEPPENFELD, *Act. Phys. Pol. B* 27 (1996) 1393.
- [3] B. PÖTTER, *Comp. Phys. Comm.* 119 (1999) 45.
- [4] S. CATANI AND M.H. SEYMOUR, *Nucl. Phys. B* 485 (1997) 291, Erratum–ibid. B 510 (1997) 503.
- [5] S. CATANI AND M.H. SEYMOUR, *Phys. Lett. B* 378 (1996) 287.
- [6] D. GRAUDENZ, preprint:, hep-ph/9710244v2, 1997.
- [7] C. DUPREL ET AL., In *these proceedings* (1999), DESY, Hamburg (Germany).
- [8] H.L. LAI ET AL., *Phys. Rev. D* 55 (1997) 1280.
- [9] T. CARLI, In *New Trends in HERA Physics* (1997), B. Kniehl and G. Kramer, Eds., Ringberg workshop, Tegernsee (Germany); MPI-PhE/97-22 and hep-ph/9709240.
- [10] S. FRIXIONE AND G. RIDOLFI, *Nucl. Phys. B* 507 (1997) 315.
- [11] M. KLASSEN AND G. KRAMER, *Phys. Lett. B* 366 (1996) 385–393.
- [12] B. PÖTTER AND G. KRAMER, *Eur. Phys. J. C* 1 (1998) 261.
- [13] H1 COLLAB., C. ADLOFF ET AL., *submitted to Eur. Phys. J.* (1998) DESY–98–076.
- [14] CDF COLLAB., F. ABE ET AL., *Phys. Rev. D* 45 (1992) 1448–1458.
- [15] S. D. ELLIS AND D. E. SOPER, *Phys. Rev. D* 48 (1993) 3160.
- [16] S. CATANI, YU. L. DOKSHITZER, M.H. SEYMOUR AND B.R. WEBBER, *Nucl. Phys. B* 406 (1993) 347–353.
- [17] H1 COLLAB., C. ADLOFF ET AL., In *XXIX Int. Conf. on HEP* (1998), paper: 520, Vancouver (Canada).
- [18] H1 COLLAB., C. ADLOFF ET AL., *Nucl. Phys. B* 545 (1999) 3.
- [19] M.H. SEYMOUR, *Nucl. Phys. B* 513 (1998) 269–300.
- [20] W.B. KILGORE AND W.T. GIELE, *Phys. Rev. D* 55 (1997) 7183–7190.
- [21] S. D. ELLIS, Z. KUNSZT AND D. E. SOPER, *Phys. Rev. Lett.* 69 (1992) 3615–3618.
- [22] B. PÖTTER AND G. KRAMER, *Phys. Lett.* 453 (1999) 295–301.



— NLO  $Q^2$  scale   
 - - - LO  $Q^2$  scale   
 ⋯ NLO  $E_T^2$  scale   
 - - - LO  $E_T^2$  scale

